



40 because of inherent instability of thin subglacial meltwater films (Kyrke-Smith et al., 2014).  
41 Numerous observations however, have highlighted preferential location of ice streams at sites  
42 of specific bed properties such as in topographic troughs, over areas of soft sedimentary  
43 geology, zones of higher geothermal heat flux or as a consequence of where subglacial  
44 meltwater is routed (Winsborrow et al., 2010; Kleiner and Humbert, 2014). These viewpoints  
45 might not be mutually exclusive if self-organisation into regularly-spaced streams is the  
46 primary control but that it is strongly mediated by local bed templates (e.g. troughs) or events  
47 (meltwater drainage) that initiate or anchor streams in certain locations. Exploring this  
48 hypothesis by numerical modelling has not yet been achieved because of uncertainties in how  
49 to formulate basal ice flow in relation to bed friction, and due to challenges of including all  
50 potentially relevant processes, especially so for subglacial water flow (Flowers, 2015).

51 Observations of spatial and temporal variations in the activity of ice streams against  
52 fluctuations in their subglacial hydrology indicate that the style and flux of water drainage is a  
53 major component driving change. Examples include: reorganisation of subglacial drainage  
54 systems (Elsworth and Suckale, 2016), subglacial water piracy (Vaughan et al., 2008; Carter et  
55 al., 2013), and development and migration of transient subglacial water pockets (Gray et al.,  
56 2005; Peters et al., 2007; Siegfried et al., 2016). However, these variations have been observed  
57 or inferred independently, at different places and on yearly timescales, thus limiting our  
58 understanding of the true role of the subglacial hydrology as primary or secondary drivers of  
59 ice stream changes. In this paper, we circumvent the challenge of numerically modelling ice  
60 stream initiation and dynamics, including subglacial water drainage, by exploiting a physical  
61 laboratory approach that simultaneously combines silicon flow, water drainage and bed erosion.

62 Connections between ice stream activity and subglacial hydrology are supported by the  
63 occurrence of geomorphic markers of meltwater drainage on ancient ice stream beds (e.g.  
64 meltwater channels, tunnel valleys, eskers) (Patterson, 1997; Margold et al., 2015; Livingstone  
65 et al., 2016). Among these markers, tunnel valleys deserve specific attention because they have  
66 high discharge capacities and, as such, may be major contributors to the release of meltwater  
67 and sediment to the ocean and may promote ice sheet stability by reducing the lubricating effect  
68 of high basal water pressure. These valleys are elongated and over-deepened hollows, ranging  
69 from a few kilometres to hundreds of kilometres long, from hundreds metres to several  
70 kilometres wide and from metres to hundreds of metres deep. Their initiation is generally  
71 attributed to subglacial meltwater erosion but their development processes (in time and space)  
72 and their relationship to ice streaming are still debated. Indeed, ice streams commonly operate  
73 because of high basal water pressure while the development of a tunnel valleys system generally  
74 leads to enhanced drainage efficiency and basal water pressure reduction (Engelhardt et al.,  
75 1990; Marciznek and Piotrowski, 2006; Kyrke-Smith et al., 2014).

76 Several field studies have already suggested a connection between catastrophic glacial  
77 outburst floods at ice sheets margins and a suite of events involving ice streaming, tunnel valley  
78 development and stagnation of the ice margin. (Jørgensen and Piotrowski, 2003; Alley et al.,  
79 2006; Hooke and Jennings, 2006; Bell et al., 2007). Such outburst floods can profoundly and  
80 rapidly alter the oceanic environment by transferring considerable amounts of ice, freshwater,

81 and sediment from continents to oceans (Evatt et al., 2006). The suspected connection between  
82 ice streams, tunnel valleys, and outburst floods have never been observed or modelled however.

83 Here, we describe the results of a physical experiment performed with an innovative  
84 analogue modelling device that provides simultaneous constraints on ice flow, subglacial  
85 meltwater drainage, subglacial sediment transport and subglacial landform development  
86 (Lelandais et al., 2016; Fig. 1). We propose that the location and initiation of ice streams might  
87 arise from subglacial meltwater pocket migration and drainage pathways and that the evolution  
88 of ice stream dynamics is subsequently controlled by subglacial drainage reorganization and  
89 tunnel valley development. This study reconciles into a single story several detached inferences,  
90 derived from observations at different timescales and at different places on modern and ancient  
91 ice streams.

## 92 2. Experimental ice stream model

93 Ice stream dynamics are controlled by various processes that act at different spatial and  
94 temporal scales; they also involve several components with complex thermo-mechanical  
95 behaviours (ice, water, till, bedrock) (Paterson, 1994). Considering all these processes and  
96 components simultaneously, together with processes of subglacial erosion, is thus a challenge  
97 for numerical computational modelling (Fowler and Johnson, 1995; Marshall, 2005; Bingham  
98 et al., 2010). Some attempts in analogue modelling have been made to improve our knowledge  
99 on subglacial erosional processes by meltwater (Catania and Paola, 2001) or gravity current  
100 instabilities produced by lubrication (Kowal and Worster, 2015). To combine ice flow  
101 dynamics and erosional aspects in a single model, we designed an alternative experimental  
102 approach that allows simultaneous modelling of ice flow, subglacial hydrology and  
103 sedimentary/geomorphic processes. With all the precautions inherent in using analogue  
104 modelling, our experiments reproduce morphologies and dynamics that compare well with  
105 subglacial landforms and ice stream dynamics despite some differences in spatial and temporal  
106 scales and a number of active processes (e.g. Paola et al., 2009).

### 107 2.1. Experimental apparatus

108 The model is set in a glass box (70 cm long, 70 cm wide and 5 cm deep) (Fig. 1). A 5 cm thick,  
109 flat, horizontal, permeable and erodible substratum, made of sand ( $d_{50}=100\ \mu\text{m}$ ) saturated with  
110 pure water and compacted to ensure homogeneous values for its density ( $\rho_{\text{bulk}} = 2000\ \text{kg/m}^3$ ),  
111 porosity ( $\Phi = 41\ \%$ ) and permeability ( $K = 10^{-4}\ \text{m/s}$ ), rests on the box floor. The ice sheet  
112 portion is modelled with a 3 cm thick layer of viscous ( $\eta = 5 \cdot 10^4\ \text{Pa s}$ ) and transparent but  
113 refractive ( $n = 1.47$ ) silicon putty placed on the substratum. The model is not designed to  
114 simulate an entire ice sheet. The silicon layer is circular in plan view (radius = 15 cm) to avoid  
115 lateral boundary effects on silicon flow. Subglacial meltwater production is simulated by  
116 injection of water with a punctual injector, 4 mm in radius, placed at a depth of 1.8 cm in the  
117 substratum and connected to a pump (Fig. 1). The injector is located below the centre of the  
118 silicon layer to be consistent with the circular geometry of the experiment. The water discharge  
119 is constant ( $1.5\ \text{dm}^3/\text{h}$ ) over the duration of the experiment and generates water flow at the  
120 silicon-substratum interface and within the substratum. Water discharge is calculated  
121 beforehand so that water pressure exceeds the combined weight of the sand and silicon layers.

122 The injection of water starts when the silicon layer reaches the dimensions we fixed for every  
123 experiment (15 cm radius and 3 cm thickness) and a perfect transparency. Once injected, water  
124 flow is divided into a Darcy flow within the substratum and a flow at the silicon/substratum  
125 interface. The water flowing at the silicon/substratum interface originates from a pipe forming  
126 at the injector once water pressure exceeds the cumulative pressure of the silicon and sand  
127 layers. The ratio between the Darcy flow and the flow at the silicon/substratum interface is  
128 inferred from computations of the water discharge flowing through the pipe based on the  
129 substratum properties and the input discharge. We estimate that 75% of the input discharge is  
130 transferred as Darcy flow in the substratum and 25% of the input discharge along the  
131 silicon/substratum interface.

## 132 2.2. Acquisition process and post-processing

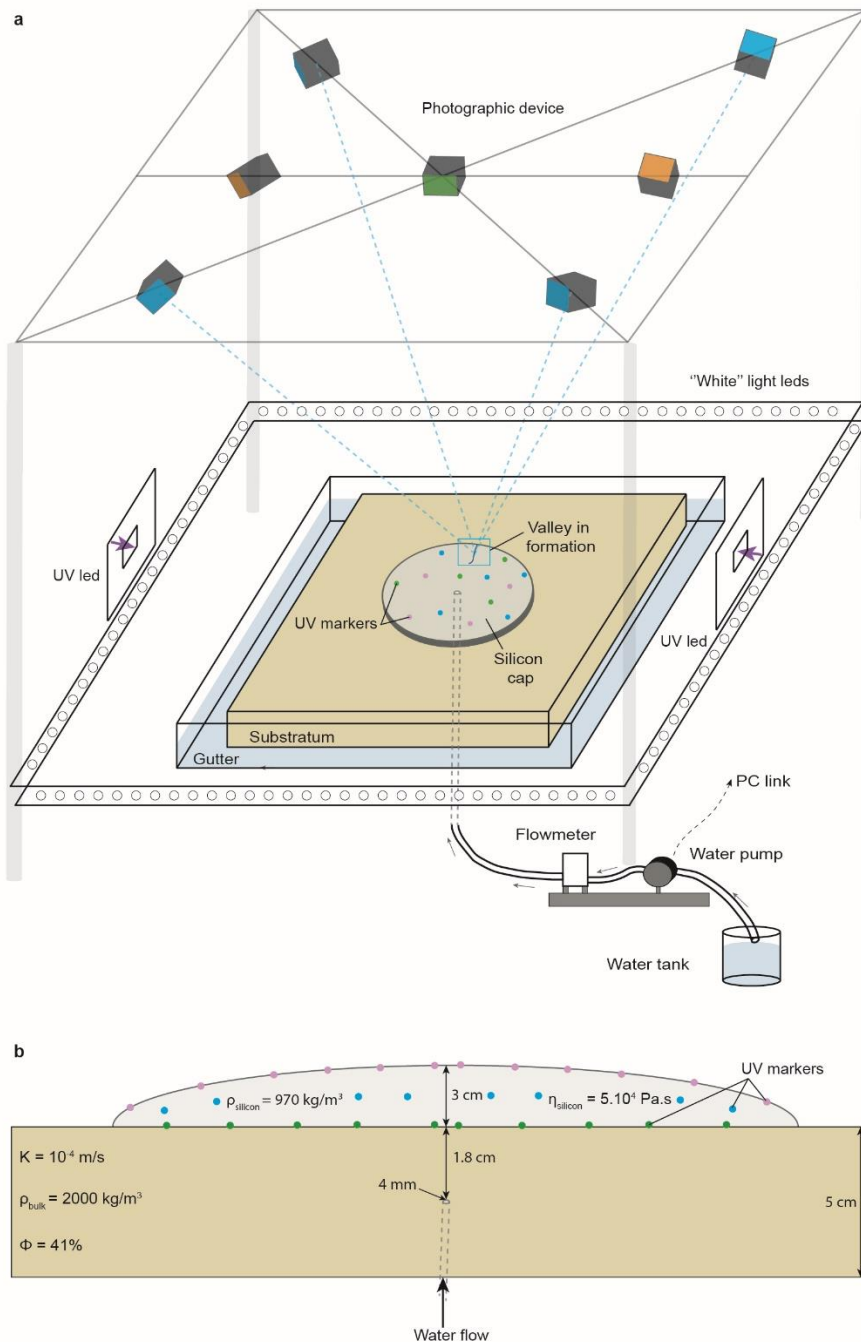
133 In order to monitor the development of landforms on the substratum, we use six  
134 synchronised cameras equidistant from the experiment centre (Fig. 1) taking photographs of the  
135 experiment every 5 seconds. Two cameras (orange on Fig. 1) cover the whole extent of the  
136 experiment and four cameras (blue on Fig. 1) focus on specific regions to obtain higher  
137 resolution images. These cameras take simultaneous pictures with differing positions and  
138 orientations. Digital elevation models of the silicon surface and of the substratum are derived  
139 from these images by photogrammetry. The ultimate stage of the experiment is to remove  
140 distortions due to light refraction through the silicon putty and apply corrections to the  
141 substratum topography. This treatment is achieved using a custom algorithm able to evaluate  
142 the gap between the measured altitude and the real altitude of each pixel of the DEM (cf detailed  
143 post-treatment methods in Lelandais et al., 2016). Tests performed on previously known  
144 topographies show that the vertical precision of the retrieved digital elevation models is better  
145 than  $10^{-1}$  mm.

146 The flow velocity of the silicon layer is monitored near its base ( $V_{\text{base}}$ ), at mid-depth ( $V_{\text{mid}}$ ) and  
147 at its surface ( $V_{\text{surface}}$ ), with an additional camera placed over the centre of the experiment (green  
148 on Fig. 1). For that purpose, the camera records the position on pictures taken at regular time  
149 intervals in ultraviolet (UV) of 180 UV paint drops (1 mm in radius) placed at 1 mm above the  
150 base, at mid-depth and at the surface of the silicon layer (Figs. 1, S1). The monitoring of every  
151 UV marker position through time was used to produce velocity and vertical displacement maps.  
152 Vertical displacement maps are interpolated from the subtraction of the DEM at time  $t$  with the  
153 DEM generated from the photographs taken a few seconds before the injection. Velocity maps  
154 are interpolated from the subtraction of the position of every marker at time  $t$  with the position  
155 of the same markers at the previous stage. These passive markers are transparent at visible  
156 wavelengths and do not alter pictures of the substratum taken through the silicon cap. They  
157 represent less than 0.5% of the silicon layer in volume and tests have shown that they do not  
158 affect its overall rheological behaviour. Uncertainties in the measured position of markers on  
159 images are less than one pixel in size (i.e. less than  $10^{-1}$  mm), thus uncertainties in the derived  
160 velocities are comprised between  $5 \cdot 10^{-4}$  and  $2 \cdot 10^{-3}$  mm/s, depending on the time interval  
161 between photographs.

162

163 2.3. Scaling and limitations

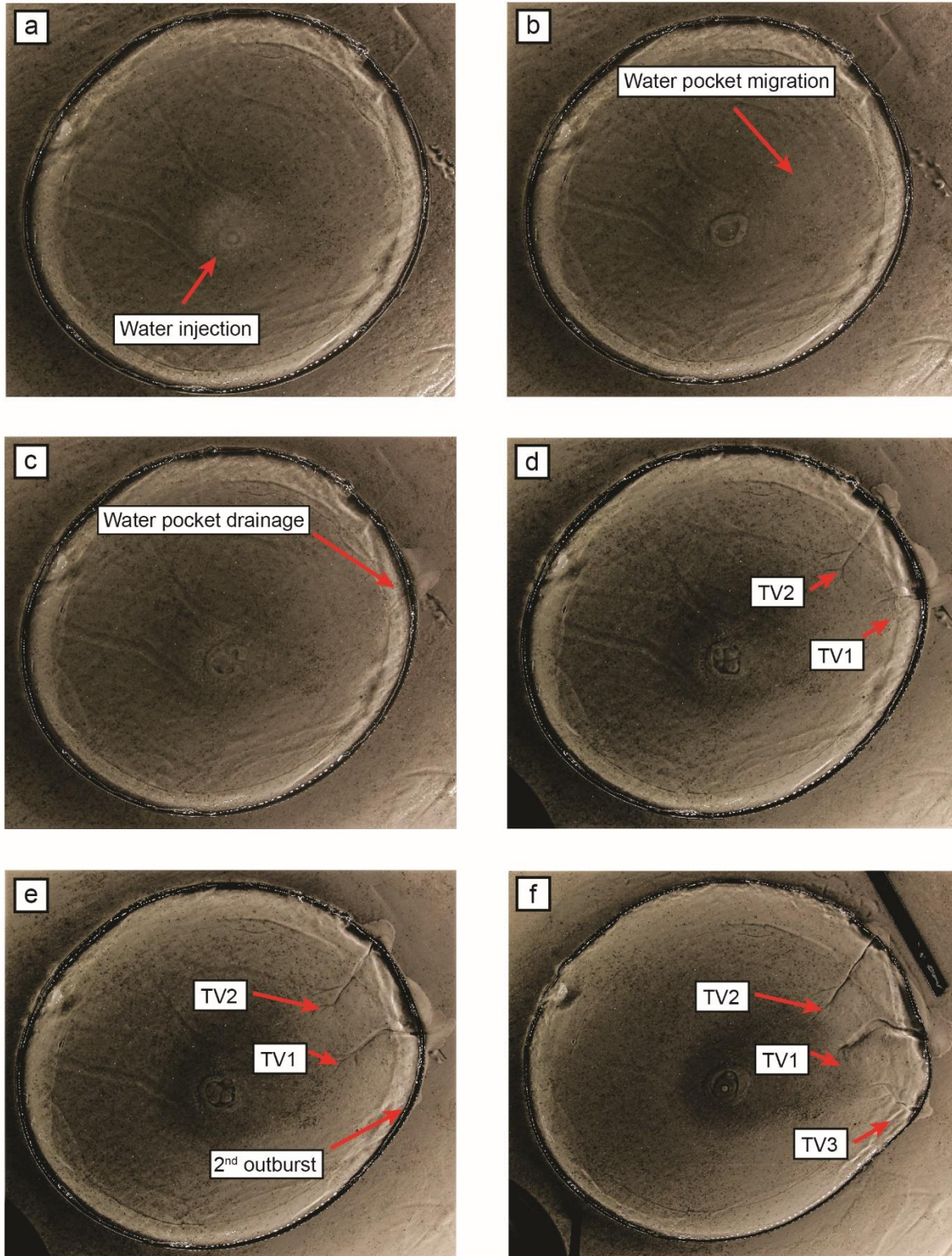
164 In this study, we focus our attention on the relations between subglacial water flow,  
165 subglacial erosion and ice flow using an experiment approach. Considering that in our model  
166 meltwater is simulated by an injection of water, the rules of a classical scaling where the model  
167 is a perfect miniaturisation of nature are not practical (Paola et al., 2009). In this perspective,  
168 we base the scaling of our model on the displacement of the natural ice and experimental silicon  
169 margins through time. We use a unit-free speed ratio between the silicon/ice margin velocity  
170 and the incision rate of experimental/natural tunnel valleys. In this way, the complexity of the  
171 relations between subglacial hydrology, subglacial erosion and ice flow, which is one of the  
172 main issue in numerical modelling, is included in the velocity values. The scaling attest that the  
173 value of the ratio between margin velocity and incision rate of tunnel valleys in the experiment  
174 fall within the field validity defined by the range of natural settings (full details in Lelandais et  
175 al., 2016). The main scaling limit regards the viscosity ratios between glacier ice, silicon putty  
176 and water. The size of the experimental ice stream, being partly controlled by the high silicon  
177 viscosity, may be underestimated compared to the size of modelled tunnel valleys.  
178 Considering that our model is a simplification of nature, we cannot simulate the whole  
179 complexity of the nature processes. In contrast with ice, the commercial silicon putty we use  
180 (Dow Corning, SGM36) is impermeable, newtonian, isotropic, and its viscosity is nearly  
181 independent of temperatures between 10 and 30°C. Therefore, rheological softening with strain  
182 rate, temperature, anisotropy, and meltwater content (e.g. Bingham et al., 2010) cannot be  
183 reproduced. The silicon putty cannot reproduce the ice/water phase transition either, requiring  
184 the use of punctual water injection in the experiment. This punctual injection does not simulate  
185 the mosaic of meltwater production regions existing beneath glaciers or the episodic input from  
186 supraglacial/englacial meltwater reservoirs. Experimental meltwater routing is predominantly  
187 controlled by the water discharge we inject in our system and therefore differs from parameters  
188 controlling hydrology in glacial systems. Subglacial meltwater routing is indeed controlled by  
189 the ice surface slope, the bed topography, and the glacier mass balance (Röthlisberger and Lang,  
190 1987). The ice surface slope controls potentiometric surfaces, generally guiding subglacial  
191 water flow parallel to ice sheet surfaces (Glen, 1954; Shreve, 1972; Fountain and Walder,  
192 1998). Finally, the substratum we use is homogeneous, flat and composed of a well-sorted  
193 mixture of sand-sized grains. This model, designed to decipher the interaction between  
194 subglacial hydrology and ice dynamics, hinders the influence of bed topography and geology  
195 (especially the influence of subglacial till) (Winsborrow et al., 2010). The deformation of the  
196 subglacial till and its complex rheological behavior is known to promote ice streaming (Alley  
197 et al., 1987), modify the subglacial hydrology, and alter the size of tunnel valleys. The  
198 development of an analogue material scaled to reproduce subglacial till characteristics is  
199 extremely difficult so we did not try to include the equivalent of a till layer in the experiment.  
200 We thus assume that the velocity contrasts observed in the experiment are likely to be amplified  
201 in natural ice sheets, by the complex rheological behaviour of ice and till. This may lead to the  
202 development of narrower ice streams with higher relative velocities and sharper lateral shear  
203 margins in natural ice sheets than in the experiment (Raymond, 1987; Perol et al., 2015).



204

205 **Figure 1.** Description of the analogue device used in this study. a, Overview of the analogue device.  
 206 The analogue device consists in a 70 cm long, 70 cm wide and 5 cm deep glass box filled with saturated  
 207 and compacted sand simulating the substratum. The ice sheet portion is simulated by a circular layer of  
 208 silicon putty containing 3 levels of UV markers. Meltwater production is simulated by a central and  
 209 punctual injection of pure water within the substratum. Five synchronized cameras placed above the  
 210 silicon putty (in blue) focus on the tunnel valley system and are used to produce digital elevation models  
 211 by photogrammetry. Another camera (in orange) takes overview photographs of the analogue device to  
 212 follow the progress of the whole experiment. A last camera (in green) is positioned at the vertical of the  
 213 silicon layer centre and is configured to take high-resolution photographs in black light of the UV  
 214 markers (illuminated with two lateral UV led lights). b, Cross-sectional profile of the analogue device  
 215 displaying the position of the UV markers and the physical characteristics of both the substratum and  
 216 the silicon layer.





217

218 **Figure 2.** Temporal evolution of the experiment seen on raw photographs. a. Formation of a water  
 219 pocket. b. Migration of the water pocket. c. Marginal drainage of the water pocket and onset of the  
 220 silicon stream. d. Development of two tunnel valleys (TV1 and TV2). e. Drainage of a second water  
 221 pocket and silicon stream migration. f. Development of a new generation of tunnel valleys (TV3) and  
 222 silicon stream decay. Silicon flow velocity and silicon surface displacement maps corresponding to the  
 223 six stages described here are presented in Figure 3.

### 224 3. Experimental results

#### 225 3.1. Stage-by-stage experimental progress

226 This experiment was repeated 12 times with identical input parameters (a 30 mm-thick silicon  
227 layer of 150 mm radius; constant water input of 1.5 dm<sup>3</sup>/h during 1800 s). After an initial  
228 identical state, a six-stage ice stream lifecycle linking outburst flooding, transitory ice  
229 streaming, and tunnel valley development has been observed for all these simulations (Figs. 2,  
230 3).

231 Initial state (Fig. S2). As long as no water is injected in the substratum, the silicon layer spreads  
232 under its own weight and displays the typical parabolic surface profile of an ice sheet. It  
233 increases in diameter and decreases in thickness with time, thus producing a radial pattern of  
234 horizontal velocities, which increase in magnitude from the centre ( $V_{\text{surface}} < 3 \cdot 10^{-3}$  mm/s) to the  
235 margin ( $V_{\text{surface}} = 8 \cdot 10^{-3}$  mm/s) (Fig. S2).  $V_{\text{base}}$  is close to 0 over the full extent of the silicon  
236 layer ( $\frac{V_{\text{base}}}{V_{\text{surface}}} \sim 0\%$ ), indicating coupling with the substratum. The silicon flow pattern changes  
237 when meltwater production is simulated by injecting water at a constant discharge (1.5 dm<sup>3</sup>/h),  
238 beneath the silicon layer.

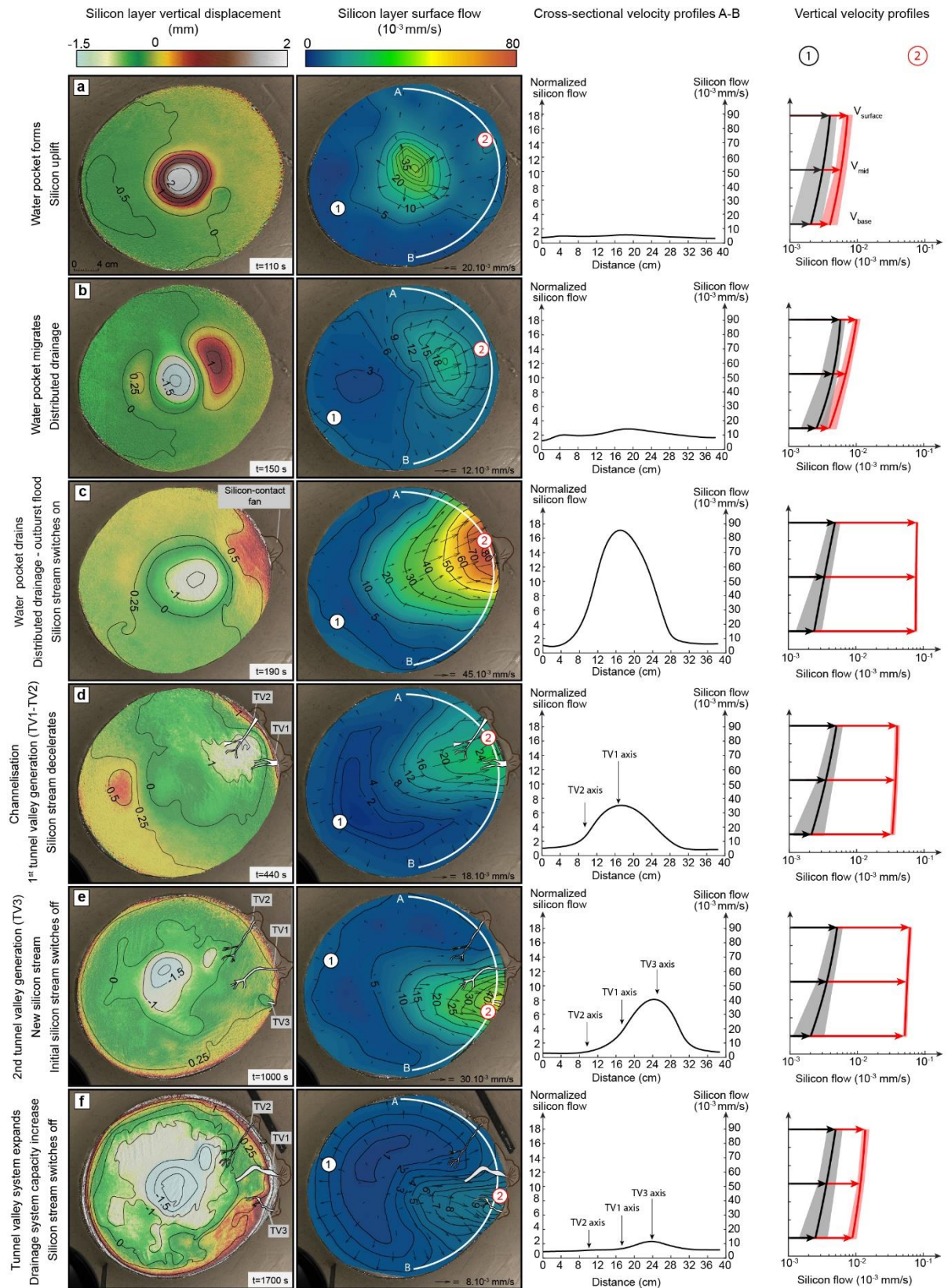
239 Stage 1 (Figs. 2a, 3a). A water pocket grows below the centre of the silicon layer and raises its  
240 surface by 2 mm. Above the water pocket, the silicon accelerates ( $V_{\text{surface}} \geq 35 \cdot 10^{-3}$  mm/s), and  
241 is decoupled from the substratum ( $\frac{V_{\text{base}}}{V_{\text{surface}}} = 75$  to 80%). Below the rest of the silicon layer,  
242 lower velocities ( $V_{\text{surface}} = 8 \cdot 10^{-3}$  mm/s,  $\frac{V_{\text{base}}}{V_{\text{surface}}} = 40$  to 50%) indicate higher basal friction.  
243 These results are consistent with inferences that meltwater ponding can form pressurised  
244 subglacial water pockets associated with basal decoupling, surface uplift, and ice flow  
245 acceleration in natural ice sheets (e.g. Hanson et al., 1998; Elsworth and Suckale, 2016;  
246 Livingstone et al., 2016). In the experiment however, these effects are restricted to an  
247 approximately circular region and are not sufficient to produce channelised ice streaming.

248 Stage 2 (Figs. 2b, 3b). The water pocket expands and migrates towards the margin of the silicon  
249 layer. The lack of channels incised in the substratum indicates that this displacement occurs as  
250 distributed water drainage without any basal erosion. In the silicon layer, the region of surface  
251 uplift, basal decoupling and acceleration ( $V_{\text{surface}} = 18 \cdot 10^{-3}$  mm/s,  $\frac{V_{\text{base}}}{V_{\text{surface}}} = 75$  to 85%)  
252 expands and migrates downstream with the water pocket. Similar migrations of pressurised  
253 subglacial water pockets have been observed or inferred under modern and ancient ice sheets  
254 (Fricker et al., 2007; Carter et al., 2017), sometimes associated with migrations of regions of  
255 ice surface uplift and ice flow acceleration (Bell et al., 2007; Stearns et al., 2008; Siegfried et  
256 al., 2016). The experiment indicates that the migration of water pockets at the ice-bed interface  
257 can contribute to the emergence of ice streams.

258

259





260

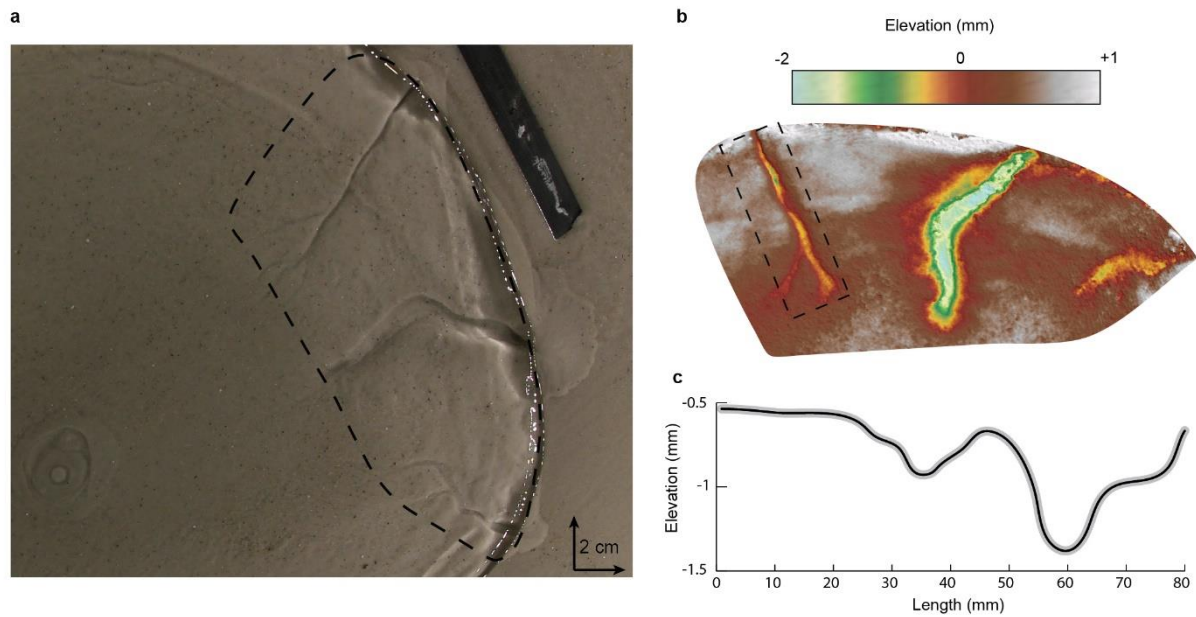
261 **Figure 3.** Temporal evolution of the experiment. a, Formation of water pocket, uplift of silicon surface  
 262 uplift and acceleration. b, Migration of water pocket and overlying region of uplift and accelerated flow.  
 263 c, Marginal drainage of water pocket and onset of silicon streaming. d, Tunnel valley development and  
 264 silicon stream deceleration. e, Formation, migration and marginal drainage of a new water pocket,

265 development of a second silicon stream and of a new tunnel valley. f, Decay of the second silicon stream.  
266 From left to right: (i) maps of vertical displacements of silicon layer surface, (ii) maps of horizontal  
267 velocity at silicon layer surface, (iii) cross-sectional velocity profiles (absolute velocity on right axis,  
268 velocity normalised by background velocity on left axis, profile locations indicated by white lines A-B  
269 on maps), (iv) vertical velocity profiles for silicon stream (red profiles, locations labelled 2 on maps)  
270 and for region opposed to silicon stream (black profiles, locations labelled 1 on maps).

271 Stage 3 (Figs. 2c, 3c). When the water pocket reaches the margin of the silicon layer, it drains  
272 suddenly as a sheet flow. This marginal outburst flood is still fed by distributed drainage and  
273 conveys sand particles eroded from the substratum towards a low-angle marginal sedimentary  
274 fan (up to 40 mm long, 30 mm wide and 0.3 mm thick; Fig. S3). Simultaneously, the silicon  
275 flow focuses in a stream (200 mm wide at the margin) that propagates upstream from the silicon  
276 margin to the water injection area. This stream immediately peaks in velocity ( $V_{\text{surface}} = 80 \cdot 10^{-3}$   
277  $\text{mm/s}$ , 16 times higher than the surrounding silicon) and is entirely decoupled from its  
278 substratum ( $\frac{V_{\text{base}}}{V_{\text{surface}}} > 90\%$ ). Although similar relations between outburst floods and ice flow  
279 accelerations have been suspected in modern (Alley et al., 2006; Bell et al., 2007; Stearns et al.,  
280 2008) and former (Livingstone et al., 2016) ice sheets, they have been documented for valley  
281 glaciers only (e.g. Anderson et al., 2005). In these regions, they can produce sudden meltwater  
282 discharges that exceed the capacity of distributed subglacial meltwater drainages and promote  
283 basal decoupling and ice flow acceleration (e.g. Magnússon et al., 2007). The experiment  
284 confirms that outburst floods can promote basal decoupling and trigger ice streaming in ice  
285 sheets (Fowler and Johnson, 1995).

286 Stage 4 (Figs. 2d, 3d). The distributed subglacial drainage system starts to channelise: two  
287 valleys (TV1 and TV2) appear below the margin of the silicon layer and gradually expand by  
288 regressive erosion of the substratum. At this stage, TV1 is 30 mm long, 12 mm wide and 0.5  
289 mm deep; TV2 is 80 mm long, 10 mm wide and 0.5 mm deep. These valleys, with their constant  
290 widths, undulating long profiles and radial distribution, are analogue to natural tunnel valleys  
291 in their dimensions, shapes, and spatial organization (Lelandais et al., 2016; Fig. 4). They are  
292 fed by distributed water drainage. The sand eroded from the substratum transits through these  
293 valleys and accumulates in high-angle marginal sedimentary fans, higher in elevation than the  
294 valley floors (TV1 fan is up to 27 mm long, 30 mm wide and 0.5 mm thick; TV2 fan is up to  
295 20 mm long, 24 mm wide and 1 mm thick; Fig. S3). In response to progressive channelisation  
296 of the water drainage into the expanding valleys, the silicon stream narrows and slows down  
297 (120 mm wide at the margin;  $V_{\text{surface}} = 24 \cdot 10^{-3} \text{ mm/s}$ ). The silicon stream, still channelised, is  
298 still flowing 8 times faster than the rest of the silicon layer and is still decoupled from the  
299 substratum ( $\frac{V_{\text{base}}}{V_{\text{surface}}} > 85\%$ ). These results are consistent with inferences that channelisation of  
300 hitherto distributed subglacial water drainage systems can occur and reduce ice flow velocity  
301 after outburst floods (Kamb, 1987; Retzlaff and Bentley, 1993; Magnússon et al., 2007), and  
302 can be responsible for narrowing and deceleration of ice streams (Raymond, 1987; Retzlaff and  
303 Bentley, 1993; Catania et al., 2006; Beem et al., 2014; Kim et al., 2016). At this stage of the  
304 experiment, this transition, which corresponds to the initiation of tunnel valleys, is not sufficient  
305 to stop ice streaming however.

306



307

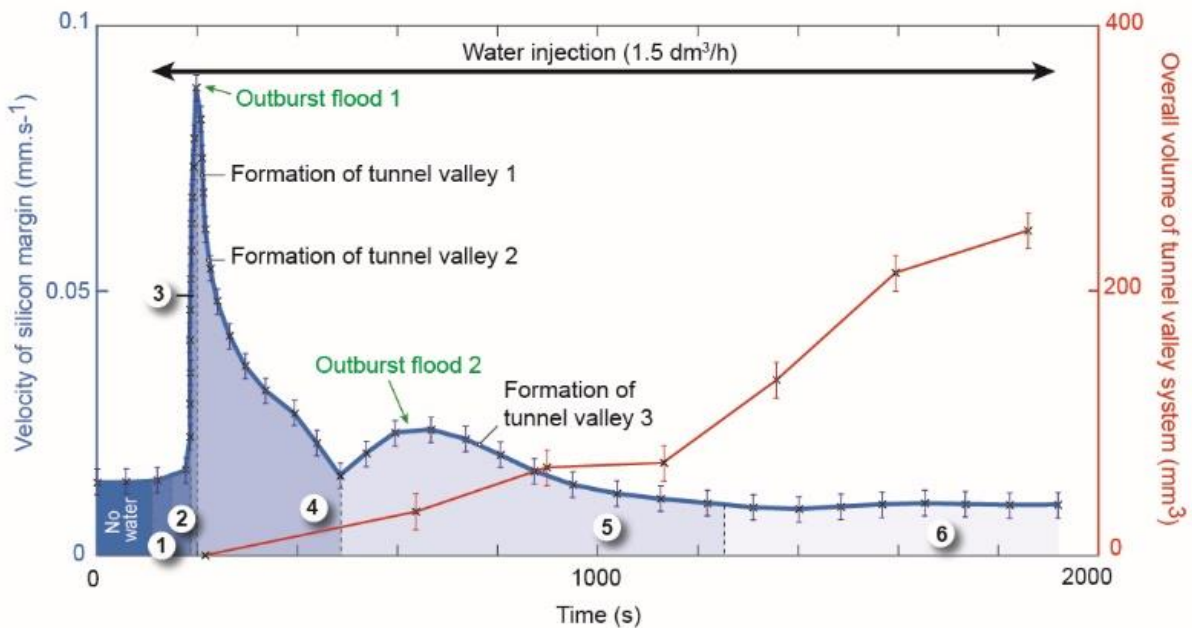
308 **Figure 4.** Digital Elevation Model (DEM) of an experimental tunnel valley and its associated  
 309 longitudinal profile. a, Snapshot of the tunnel valley system. b, DEM of the tunnel valley corresponding  
 310 to the one highlighted by a dashed box in a. c, Undulating longitudinal profile of the tunnel valley bottom  
 311 extracted from the DEM in the dashed box shown in b.

312 Stage 5 (Figs. 2e, 3e). A new transient water pocket grows below the silicon layer, migrates and  
 313 drains as an outburst flood, thus forming a new low-angle marginal sedimentary fan with at  
 314 lateral offset of 4 cm with respect to TV1. This induces the activation of a second stream ( $V_{\text{surface}}$   
 315  $= 40 \cdot 10^{-3}$  mm/s) decoupled from its substratum ( $\frac{V_{\text{base}}}{V_{\text{surface}}} = 80\%$ ) and the initiation of a new  
 316 radial valley (TV3), in a hitherto slow-moving region of the silicon cap. Simultaneously, the  
 317 first silicon stream switches off ( $V_{\text{surface}} = 10 \cdot 10^{-3}$  mm/s), and recouple to its substratum  
 318 ( $\frac{V_{\text{base}}}{V_{\text{surface}}} = 30\%$ ), but water and sand still flow through TV1 and TV2. At this stage, TV1 is  
 319 100 mm long, 8 mm wide and 0.7 mm deep and its fan is up to 21 mm long, 40 mm wide, and  
 320 1.1 mm thick; TV2 is 80 mm long, 7.5 mm wide, and 0.6 mm deep and its fan is up to 20 mm  
 321 long, 28 mm wide, and 1.6 mm thick. This result is consistent with inferences that natural ice  
 322 streams can switch on and off, surge, and jump in location in response to changes in subglacial  
 323 water drainage reorganisation (Catania et al., 2012; Le Brocq et al., 2013; Beem et al., 2014;  
 324 Hulbe et al., 2016). The experiment further indicates that this complex behaviour is controlled  
 325 by the growth and migration, in various possible directions, of transient pressurised subglacial  
 326 water pockets that form successively as long as the discharge capacity of tunnel valleys systems  
 327 is not sufficient to drain efficiently the available meltwater.

328 Stage 6 (Figs. 2f, 3f). Since their initiation, TV1, TV2, and TV3 have progressively increased  
 329 in width, depth and length. At this stage TV1 is 100 mm long, 17 mm wide, and 1.2 mm deep  
 330 and its fan is 28 mm long, 4 mm wide, and 1.5 mm high at the maximum; TV2 is 80 mm long,  
 331 10 mm wide, and 0.8 mm deep and its fan is up to 16 mm long, 23 mm wide and 1.6 mm thick  
 332 ; TV3 is 60 mm long, 11 mm wide, and 0.55 mm deep and its fan is up to 14 mm long, 23 mm  
 333 wide, and 0.7 mm thick. Their overall volume and discharge capacity have thus increased (Fig.  
 334 5). In response to this increased drainage efficiency, the second stream gradually decays ( $V_{\text{surface}}$



335  $= 5 \cdot 10^3 \text{ mm} \cdot \text{s}^{-1}$ ), and recouples to its substratum ( $\frac{V_{base}}{V_{surface}} = 35\%$ ). The silicon layer ultimately  
 336 recovers a radial flow pattern (Fig. 3f). This result is consistent with the inference that ice  
 337 streams may decelerate and even switch off in response to reduction of subglacial water  
 338 pressures when efficient subglacial water drainage systems develop (Retzlaff and Bentley,  
 339 1993; Beem et al., 2014; Livingstone et al., 2016; Kim et al., 2016). In the experiment, this  
 340 development is governed by the expansion of tunnel valley networks. Large glaciotectonic  
 341 thrust masses at the ice margin near tunnel valley fans are generally assumed to be field  
 342 evidence of a fast ice flow stage prior to drainage through tunnel valleys (Hooke and Jennings,  
 343 2006).



344  
 345 **Figure 5.** Progressive expansion of overall volume of tunnel valleys system vs. velocity of silicon  
 346 margin through the experiment. The circled numbers correspond to the six-stages of the proposed ice  
 347 stream lifecycle.

### 348 3.2. Experimental reproducibility and variability

349 This experiment has been reproduced 12 times with identical input parameters. We always  
 350 observe the same processes and events acting in a similar chronological order : (1) water pocket  
 351 forms; (2) water pocket migrates; (3) water pocket drains (outburst flood) and silicon stream  
 352 switches on; (4) Tunnel valleys form in response to channelisation; (5) silicon stream slows  
 353 down and (6) finally switches off in response to the increase of drainage efficiency during  
 354 tunnel valley development. However, despite this consistency in the progress of all simulations  
 355 some variability has been detected. We measured different migration rates for the water pocket  
 356 ranging from 30 s to 80 s that may result from small changes in subglacial topography and in  
 357 the dynamics of silicon-bed decoupling. Considering a constant water discharge and the  
 358 characteristics of the experiment, a longer period of migration implies: a longer period of water  
 359 storage and a bigger water volume released at the silicon margin during the pocket drainage  
 360 .We therefore recorded peak velocities for water pocket drainage ranging from  $6 \cdot 10^{-3}$  to  $12 \cdot 10^{-3}$   
 361  $\text{mm/s}$ . In response to variations of the water volume drained at the margin and peak discharge,

362 the maximum width of the silicon stream varies from 120 to 250 mm. The magnitude of the  
363 outburst flood triggered during water pocket drainage also influences the amount of tunnel  
364 valleys that subsequently form during the channelisation stage. A high magnitude outburst flood  
365 generates a wider erosion beneath the silicon that will be suitable for the development of  
366 multiple tunnel valleys. Hence, the amount of tunnel valleys at the end of the experiments  
367 ranged from 1 to 5 with 1 to 3 tunnel valleys formed simultaneously during the initiation of the  
368 channelisation stage. These valleys range from 40 to 120 mm long, 3 to 18 mm wide, and 0.3  
369 to 1.8 mm deep. During tunnel valleys development, the evolution of drainage efficiency varies  
370 between the experiments. A relatively inefficient system of tunnel valleys induces upstream  
371 water pocket formation. As observed in Figure 3e, the drainage of this belated water pocket  
372 may provoke water re-routing beneath the silicon layer and subsequent lateral migration of the  
373 silicon stream. We counted 0 to 2 events of silicon stream migration for single experiments.  
374 Finally, the time required to reach the phase of ice stream decay highly depends on the amount  
375 of tunnel valleys formed during the experiments and their progressive development. We  
376 observed a lifetime for the silicon stream ranging from 500 s to 1700 s, correlated with the  
377 evolution of the drainage efficiency during tunnel valley development.

#### 378 4. Proposed lifecycle of transitory ice streams

379 The experiment demonstrates that, on flat and homogenous beds, ice streams may arise,  
380 progress, and decay in response to mechanical interactions between ice flow, subglacial water  
381 drainage, and bed erosion. On uneven or heterogeneous beds (not simulated in this model),  
382 these interactions may additionally be enhanced or disturbed by spatial variations in the  
383 subglacial topography, geology, and geothermal heat flux (e.g. Bentley, 1987; Blankenship et  
384 al., 1993; Anandakrishnan et al., 1998; Bourgeois et al., 2000; Winsborrow et al., 2010). The  
385 complex rheology of glacial ice and subglacial till (both generally soften with increasing strain  
386 rate, temperature, water content, and anisotropy) may also enhance these interactions by  
387 increasing velocity contrasts between ice streams and their slower-moving margins. This may  
388 lead to the development of narrower ice streams with higher velocities and sharper lateral shear  
389 margins in natural ice sheets than in the experiment (Raymond, 1987; Perol et al., 2015).

390 Although the complexity of glacial systems cannot be fully modelled using the present  
391 experimental setup, our results highlight the critical connection between ice streams and tunnel  
392 valleys. As reviewed in Kehew et al., (2012) and suggested in Ravier et al., (2015) this relation  
393 was suspected from the occurrence of tunnel valleys on ancient ice streams beds. However, it  
394 raised a contradiction: subglacial meltwater pressures are generally supposed to be high below  
395 ice streams (Bennett, 2003) while tunnel valleys are generally assumed to operate at lower water  
396 pressures (Marczinek and Piotrowski, 2006). Although speculated from field evidences, our  
397 results demonstrate that ice streaming, tunnel valley formation, release of marginal outburst  
398 floods and subglacial water drainage reorganization may be interdependent parts of a single ice  
399 stream lifecycle that involves temporal changes in subglacial meltwater pressures (Fig. 6).

400 1. Ice stream seeding. A prerequisite to the activation of ice streams is the formation of  
401 pressurised subglacial pockets by meltwater ponding in ice sheet hinterlands. Approximately  
402 circular regions of surface uplift and accelerated ice flow develop above these transient water  
403 pockets.

404 2. Ice stream gestation. Pressurised water pockets migrate downstream by distributed water  
405 flow. Regions of surface uplift and accelerated ice flow migrate accordingly.

406 3. Ice stream birth. Once water pockets reach ice sheet margins, they drain as outburst floods.  
407 At that time, ice streams switch on, peak in velocity, and propagate towards ice sheet hinterlands  
408 as decoupled corridors of accelerated ice flow underlain by pressurised distributed water  
409 drainage.

410 4. Ice stream aging. Subglacial water drainage then channelises gradually: tunnel valleys fed  
411 by pressurised distributed drainage start to form at ice stream fronts. Subsequent expansion of  
412 tunnel valleys by regressive erosion progressively increases their overall discharge capacity,  
413 lowers subglacial water pressures and provokes gradual ice stream recoupling and deceleration.  
414 The response of ice stream dynamics to drainage channelisation and tunnel valley development  
415 might be underestimated due to the high erodability of the subglacial bed used in the  
416 experiment.

417 5. Ice stream rebirth (relocation or surge). As long as tunnel valley systems keep low drainage  
418 capacities, successive pressurised subglacial water pockets can form, migrate, and drain as  
419 marginal outburst floods. On even and homogeneous ice sheet beds, the subglacial water  
420 drainage is controlled by the surface topography of ice sheets: subtle temporal changes in this  
421 topography may thus be able to produce consecutive generations of ice streams and tunnel  
422 valleys at different locations and with different flow directions. These jumps in locations and  
423 directions may be responsible for the formation of independent, but sometimes intersecting, ice  
424 streams corridors and tunnel valleys networks on some ancient ice sheet beds (Fowler and  
425 Johnson, 1995; Jørgensen and Piotrowski, 2003). By contrast, if subglacial water routes and ice  
426 flow are constrained by bed heterogeneities, migration of successive subglacial water pockets  
427 along predetermined paths may induce sequential ice stream surges (Fowler and Johnson, 1995;  
428 Hulbe et al., 2016) and participate in the gradual development of complex tunnel valley systems  
429 at fixed places, like the Dry Valleys “Labyrinth” in Antarctica (Lewis et al., 2006).

430 6. Ice stream senescence. Ice streams may ultimately switch off when drainage capacities of  
431 tunnel valley systems are sufficient to limit subglacial water overpressures. The progressive  
432 decay of an ice stream activity can be partially produced by the thinning of the ice layer and the  
433 subsequent reduction of the stress driving ice flow in ice stream corridors (Robel et al., 2013).  
434 Our experiments display negligible thinning prior to ice stream decay. A constant water  
435 discharge being applied in experiments, we demonstrate that increased drainage efficiency  
436 during tunnel valley development can solely be responsible for ice stream slowdown. Tunnel  
437 valleys and ice streams are frequently found to co-exist as exemplified by the many examples  
438 reported from the southern margin of the Laurentide Ice Sheet (Patterson, 1997; Livingstone  
439 and Clark, 2016). In one case, development of tunnel valleys has been suggested to have led to  
440 stagnation of ice flow at an ice stream terminus (Patterson, 1997), a process that we have now  
441 demonstrated by modelling. This further indicates that tunnel valleys development could secure  
442 ice sheet stability as hinted by Marczynek and Piotrowski, (2006) by preventing ice stream  
443 destabilisation. We apply a constant meltwater discharge to our model, however meltwater  
444 production and discharge in a subglacial system fluctuates at different time scales (day, year,  
445 decades). Fluctuating water production may have further implication on the size of ice streams,



446 the size and amount of tunnel valleys that develop through time, and the timescale involved in  
447 ice sheet destabilization and stabilization. The oscillation in water production could strengthen  
448 and multiply the life cycles of some transitory ice streams, already deciphered with a constant  
449 water discharge in this study.

450 In a global change context, phenomena of ice stream stabilisation would requires that pre-  
451 existing and newly forming tunnel valley systems expand sufficiently fast to accommodate  
452 increased meltwater production. Investigating the processes and rates of tunnel valley  
453 development are more than ever warranted to better assess ancient and present-day ice sheets  
454 behaviour.

455

456

457

458

459

460

461

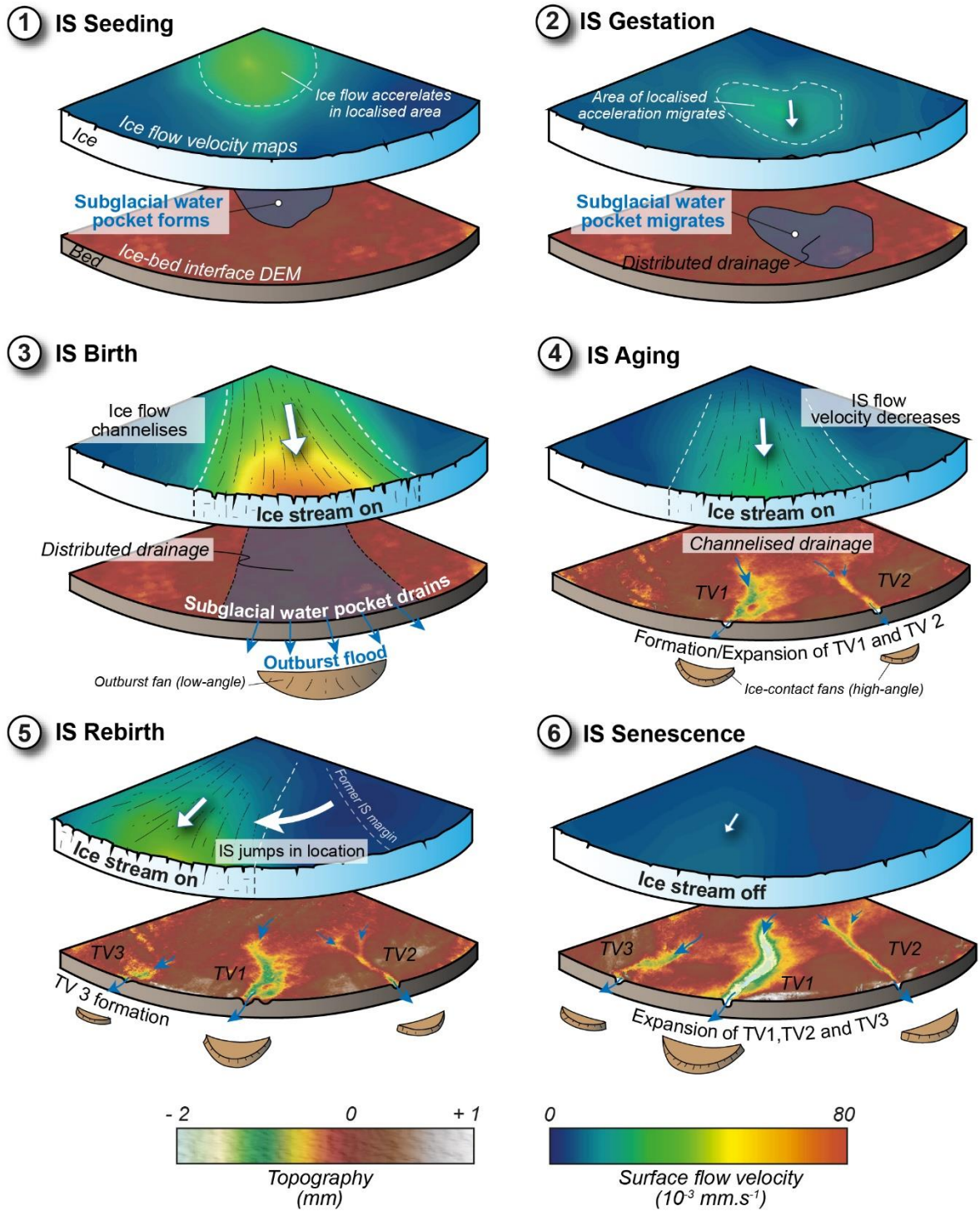
462

463

464

465

466



467

468 **Figure 6.** Chronological sequence with interpretative sketches illustrating the proposed ice stream lifecycle and the relations with tunnel valley development. Basal topography and surface  
 469 ice stream lifecycle and the relations with tunnel valley development. Basal topography and surface  
 470 flow velocity maps are derived from the experiment.

471

472

473

474 5. Conclusion

475 The transitory and mobile nature of ice streams may be understood in the framework of a  
476 model lifecycle that involves temporal changes in subglacial meltwater pressures and arises  
477 from interactions between ice flow, subglacial water drainage and bed erosion. In this model  
478 lifecycle transitory ice streams arise, progress and decay in response to subglacial flooding,  
479 changes in type and efficiency of subglacial drainage, and development of tunnel valleys. These  
480 results are consistent with (and reconcile) a variety of otherwise detached observations  
481 performed at different timescales and at different places, on modern and ancient natural ice  
482 streams. One of the most novel outcomes of this study, is that subglacial tunnel valley  
483 development may be crucial in controlling ice stream vanishing and perhaps, as a consequence,  
484 in preventing catastrophic ice sheet collapses during periods of climate change. The processes  
485 and rates of tunnel valley development are thus major issues for predicting the forthcoming  
486 behaviour of present-day ice sheets and for assessing their contribution to the release of ice and  
487 freshwater to the ocean. The innovative experimental approach, used here opens new  
488 perspectives on the understanding of subglacial processes controlling ice sheet dynamics and  
489 destabilisation.

490 **Author contributions:**

491 OB, RM, ER and SP conceived this research and gathered funding. TL designed and conducted  
492 the experiments (setup, monitoring and post-treatment), with contributions by RM and PS. TL,  
493 ER, OB, CDC, SP and RM contributed to the interpretation of the results and of their natural  
494 implications. TL wrote the first draft of the manuscript; ER, OB, SP and CDC contributed  
495 substantially to its present version.

496 **Competing interests:**

497 The authors declare that they have no conflict of interest

498 **Acknowledgements:**

499 This study is part of the DEFORm project (Deformation and Erosion by Fluid Overpressure)  
500 funded by “Région Pays de la Loire”. Additional financial support was provided by the French  
501 “Agence Nationale de la Recherche” through grant ANR-12-BS06-0014 ‘SEQSTRAT-ICE’  
502 and the “Institut National des Sciences de l’Univers” (INSU) through the ‘Programme National  
503 de Planétologie’ (PNP) and ‘Système Terre : Processus et Couplages’ (SYSTER) programs.

504 **References**

- 505 Alley, R. B., Blankenship, D. D., Rooney, S. T. and Bentley, C. R.: Till beneath ice stream B:  
506 4. A coupled ice-till flow model, *J. Geophys. Res. Solid Earth.*, 92, 8931–8940, doi:  
507 10.1029/JB092iB09p08931, 1987.  
508  
509 Alley, R. B., Dupont, T. K., Parizek, B. R., Anandkrishnan, S., Lawson, D. E., Larson, G. J.,  
510 and Evenson, E. B.: Outburst flooding and the initiation of ice-stream surges in response to  
511 climatic cooling: A hypothesis, *Geomorphology.*, 75, 76–89,  
512 doi:10.1016/j.geomorph.2004.01.011, 2006.

513  
514 Anandakrishnan, S., Blankenship, D. D., Alley, R. B., and Stoffa, P. L.: Influence of subglacial  
515 geology on the position of a West Antarctic ice stream from seismic observations, *Nature.*,  
516 394(6688), 62–65, doi: 10.1038/27889, 1998.

517  
518 Anderson, R. S., Walder, J. S., Anderson, S. P., Trabant, D. C. and Fountain, A. G.: The  
519 dynamic response of Kennicott Glacier , Alaska , USA , to the Hidden Creek Lake outburst  
520 flood, *Annals of Glaciology.*, 40, 237–242, doi: 10.3189/172756405781813438, 2005.

521  
522 Bamber, J. L., Vaughan, D. G. & Joughin, I.: Widespread Complex Flow in the Interior of the  
523 Antarctic Ice Sheet, *Science.*, 287, 1248–1250, doi: 10.1126/science.287.5456.1248, 2000.

524  
525 Beckley, B.; Zelensky, N.P.; Holmes, S.A.;Lemoine, F.G.; Ray, R.D.; Mitchum, G.T.; Desai,  
526 S.; Brown, S.T.. 2015. Global Mean Sea Level Trend from Integrated Multi-Mission Ocean  
527 Altimeters TOPEX/Poseidon Jason-1 and OSTM/Jason-2 Version 3. Ver. 3. PO.DAAC, CA,  
528 USA. Dataset accessed at <http://dx.doi.org/10.5067/GMSLM-TJ123>.

529  
530 Beem, L. H., Tulaczyk, S. M., King, M. A., Bougamont, M., Fricker, H. A., and Christoffersen,  
531 P.: Variable deceleration of Whillans Ice Stream, West Antarctica, *J. Geophys. Res. Earth Surf.*,  
532 119, 212–224, doi: 10.1002/2013JF002958, 2014.

533  
534 Bell, R. E., Studinger, M., Shuman, C. A., Fahnestock, M. A. and Joughin, I.: Large subglacial  
535 lakes in East Antarctica at the onset of fast-flowing ice streams, *Nature.*, 445, 904–907, doi:  
536 10.1038/nature05554, 2007.

537  
538 Bennett, M. R.: Ice streams as the arteries of an ice sheet: their mechanics, stability and  
539 significance, *Earth-Science Rev.*, 61, 309–339, doi: 10.1016/S0012-8252(02)00130-7, 2003.

540  
541 Bentley, C. R.: Antarctic ice streams: a review. *J. Geophys. Res. Solid Earth.*, 92(B9), 8843–  
542 8858, doi: 10.1029/JB092iB09p08843, 1987.

543  
544 Bingham, R. G., King, E. C., Smith, A. M. and Pritchard, H. D.: Glacial geomorphology:  
545 towards a convergence of glaciology and geomorphology, *Prog. Phys. Geogr.*, 34, 327–355,  
546 doi: 10.1177/0309133309360631, 2010.

547  
548 Blankenship, D. D., Bell, R. E., Hodge, S. M., Brozena, J. M., Behrendt, J. C., and Finn, C. A.:  
549 Active volcanism beneath the West Antarctic ice sheet and implications for ice-sheet stability,  
550 *Nature.*, 361(6412), 526–529, doi: 10.1038/361526a0, 1993.

551  
552 Bourgeois, O., Dauteuil, O., and Van Vliet-Lanoe, B.: Geothermal control on flow patterns in  
553 the Last Glacial Maximum ice sheet of Iceland, *Earth Surf. Process and Landforms.*, 25, 59–  
554 76, doi: 10.1002/(SICI)1096-9837(200001)25:1<59::AID-ESP48>3.0.CO;2-T, 2000.

555  
556 Carter, S. P., Fricker, H. A., and Siegfried, M. R.: Evidence of rapid subglacial water piracy  
557 under Whillans Ice Stream, West Antarctica, *Journal of Glaciology.*, 59, 1147–1162, doi:  
10.3189/2013JoG13J085, 2013.

558

559 Carter, S. P., Fricker, H. A., and Siegfried, M. R.: Antarctic subglacial lakes drain through  
560 sediment-floored canals: Theory and model testing on real and idealized domains, *Cryosph.*,  
561 **11**, 381–405, doi: 10.5194/tc-11-381-2017, 2017.

562

563 Catania, G., and Paola, C.: Braiding under glass, *Geology.*, **29**, 259–262, doi: 10.1130/0091-  
564 7613(2001)029<0259:BUG>2.0.CO;2, 2001.

565

566 Catania, G. A., Scambos, T. A., Conway, H., and Raymond, C. F.: Sequential stagnation of  
567 Kamb ice stream, West Antarctica, *Geophys. Res. Lett.*, **33**(14), L14502 doi:  
568 10.1029/2006GL026430, 2006.

569

570 Catania, G., Hulbe, C., Conway, H., Scambos, T. A., and Raymond, C. F.: Variability in the  
571 mass flux of the Ross ice streams, West Antarctica, over the last millennium. *J. Glaciol.* **58**,  
572 741–752, doi: 10.3189/2012JoG11J219, 2012.

573

574 Elsworth, C. W., and Suckale, J.: Rapid ice flow rearrangement induced by subglacial drainage  
575 in West Antarctica, *Geophys. Res. Lett.*, **43**, 697–707, doi: 10.1002/2016GL070430, 2016.

576

577 Engelhardt, H., Humphrey, N., Kamb, B., and Fahnestock, M.: Physical conditions at the base  
578 of a fast moving antarctic ice stream, *Science.*, **248**(4951), 57–59, doi:  
579 10.1126/science.248.4951.57, 1990.

580

581 Evatt, G. W., Fowler, A. C., Clark, C. D., and Hulton, N. R. J.: Subglacial floods beneath ice  
582 sheets, *Philos. Trans. R. Soc. London A Math. Phys. Eng. Sci.*, **364**, 1769–1794, doi:  
583 10.1098/rsta.2006.1798, 2006.

584

585 Flowers, G. E.: Modelling water flow under glaciers and ice sheets, *Proc. R. Soc. A Math. Phys.*  
586 *Eng. Sci.*, **471**(2176), 20140907, doi: 10.1098/rspa.2014.0907, 2015.

587

588 Fountain, A. G., and Walder, J. S.: Water flow through temperate glaciers, *Rev. Geophys.*, **36**,  
299–328, doi: 10.1029/97RG03579, 1998.

589

590 Fowler, A. C., and Johnson, C.: Hydraulic run-away: a mechanism for thermally regulated  
surges of ice sheets, *J. Glaciol.*, **41**, 454–461, doi: 10.3189/S002214300003478X, 1995.

591

592 Fricker, H. A., Scambos, T., Bindshadler, R., and Padman, L.: An active subglacial water  
593 system in West Antarctica mapped from space, *Science.*, **315**, 1544–1548, doi:  
10.1126/science.1136897, 2007.

594

595 Glen, J. W.: The stability of ice-dammed lakes and other water-filled holes in glaciers. *Journal*  
*of Glaciology*, **2**(15), 316–318, doi: 10.3189/S0022143000025132, 1954.

596

597 Gray, L., Joughin, I., Tulaczyk, S., Spikes, V. B., Bindshadler, R., and Jezek, K.: Evidence for  
598 subglacial water transport in the West Antarctic Ice Sheet through three-dimensional satellite  
599 radar interferometry, *Geophys. Res. Lett.*, **32**, L03501, doi: 10.1029/2004GL021387, 2005.

600

601 Hanson, B., Hooke, R. L., and Grace, E. M.: Short-term velocity and water-pressure variations  
602 down-glacier from a riegel, Storglaciären, Sweden. *Journal of Glaciology*, **44**(147), 359–367,  
doi: 10.3189/S0022143000002689, 1998).

603 Hindmarsh, R. C. A.: Consistent generation of ice-streams via thermo-viscous instabilities  
604 modulated by membrane stresses, *Geophys. Res. Lett.*, 36, L06502, doi:  
605 10.1029/2008GL036877, 2009.  
606

607 Hooke, R. L., and Jennings, C. E.: On the formation of the tunnel valleys of the southern  
608 Laurentide ice sheet, *Quat. Sci. Rev.*, 25, 1364–1372, doi: 10.1016/j.quascirev.2006.01.018,  
609 2006.  
610

611 Hulbe, C.: Is ice sheet collapse in West Antarctica unstoppable?, *Science.*, 356, 910–911, doi:  
612 10.1126/science.aam9728, 2017.  
613

614 Hulbe, C. L., Scambos, T. A., Klinger, M., and Fahnestock, M. A.: Flow variability and ongoing  
615 margin shifts on Bindschadler and MacAyeal Ice Streams, West Antarctica, *J. Geophys. Res.*  
616 *Earth Surf.*, 121, 283–293, doi: 10.1002/2015JF003670, 2016.  
617

618 Jørgensen, F., and Piotrowski, J. A.: Signature of the Baltic ice stream on Funen Island,  
619 Denmark during the Weichselian glaciation, *Boreas.*, 32, 242–255, doi: 10.1111/j.1502-  
620 3885.2003.tb01440.x, 2003.  
621

622 Kamb, B.: Glacier surge mechanism based on linked cavity configuration of the basal water  
623 conduit system, *J. Geophys. Res. Solid Earth.*, 92, 9083–9100, doi: 10.1029/JB092iB09p09083,  
624 1987.  
625

626 Kehew, A. E., Piotrowski, J. A., and Jørgensen, F.: Tunnel valleys: Concepts and controversies.  
627 A review, *Earth-Science Rev.*, 113, 33–58, doi: 10.1016/j.earscirev.2012.02.002, 2012.  
628

629 Kim, B.-H., Lee, C.-K., Seo, K.-W., Lee, W. S., and Scambos, T.: Active subglacial lakes  
630 beneath the stagnant trunk of Kamb Ice Stream: evidence of channelized subglacial flow,  
631 *Cryosph.*, 10, 2971–2980, <https://doi.org/10.5194/tc-10-2971-2016>, 2016.  
632

633 Kleiner, T., and Humbert, A.: Numerical simulations of major ice streams in western  
634 Dronning Maud Land, Antarctica, under wet and dry basal conditions, *J. Glaciol.*, 60, 215–  
635 232, doi: 10.3189/2014JoG13J006, 2014.

636 Kowal, K. N., and Worster, M. G.: Lubricated viscous gravity currents, *Journal of Fluid*  
637 *Mechanics.*, 766, 626–655, doi: 10.1017/jfm.2015.30, 2000.

638 Kyrke-Smith, T.M., Katz, R.F., and Fowler, A.C.: Subglacial hydrology and the formation of  
639 ice streams, *Proceedings of the Royal Society.*, A 470(2161), 20130494, doi:  
640 10.1098/rspa.2013.0494, 2014.  
641

642 Le Brocq, A. M., Ross, N., Griggs, J.A., Bingham, R.G., Corr, H.F.J., Ferraccioli, F., Jenkins,  
643 A., Jordan, T.A., Payne, A.J., Rippin, D.M., and Siegert, M.J.: Evidence from ice shelves for  
644 channelized meltwater flow beneath the Antarctic Ice Sheet, *Nat. Geosci.*, 6, 945–948, doi:  
645 10.1038/ngeo1977, 2013.  
646

647 Lelandais, T., Mourgues, R., Ravier, É., Pochat, S., Strzeczynski, P., and Bourgeois, O.:  
648 Experimental modeling of pressurized subglacial water flow: Implications for tunnel valley  
649 formation, *J. of Geophy. Res. Earth Surface.*, 121(11), 2022–2041, doi: 10.1002/2016JF003957,  
650 2016.  
651



652 Lewis, A. R., Marchant, D. R., Kowalewski, D. E., Baldwin, S. L., and Webb, L. E.: The age  
653 and origin of the Labyrinth, western Dry Valleys, Antarctica: Evidence for extensive middle  
654 Miocene subglacial floods and freshwater discharge to the Southern Ocean, *Geology.*, 34,  
655 513–516, doi: 10.1130/G22145.1, 2006.

656 Livingstone, S. J., and Clark, C. D.: Morphological properties of tunnel valleys of the southern  
657 sector of the Laurentide Ice Sheet and implications for their formation, *Earth Surface*  
658 *Dynamics*,4,567-589, doi: 10.5194/esurf-4-567-2016, 2016.

659

660 Livingstone, S. J., Utting, D. J., Ruffell, A., Clark, C. D., Pawley, S., Atkinson, N., and Fowler,  
661 A. C.: Discovery of relict subglacial lakes and their geometry and mechanism of drainage. *Nat.*  
662 *Commun.*, 7,11767, doi: 10.1038/ncomms11767, 2016.

663

664 Magnússon, E., Rott, H., Björnsson, H., and Pálsson, F., The impact of jökulhlaups on basal  
665 sliding observed by SAR interferometry on Vatnajökull, Iceland, *J. Glaciol.*, 53, 232–240,  
666 doi: 10.3189/172756507782202810, 2007.

667 Marciznek, S., and Piotrowski, J. A.: Groundwater flow under the margin of the last  
668 Scandinavian ice Sheet Around the EckernföRde Bay, Northwest Germany, *Glacier Sci.*  
669 *Environ. Chang.*, Knight, P.G., Blackwell Science Ltd 60–62, doi:  
670 10.1002/9780470750636.ch10, 2006.

671 Margold, M., Stokes, C. R., Clark, C. D., and Kleman, J.: Ice streams in the Laurentide Ice  
672 Sheet: a new mapping inventory, *J. Maps.*, 11, 380–395, doi: 10.1080/17445647.2014.912036,  
673 2015.

674 Marshall, S. J.: Recent advances in understanding ice sheet dynamics, *Earth Planet. Sci. Lett.*,  
675 240, 191–204, doi: 10.1016/j.epsl.2005.08.016, 2005.

676 Paola, C., Straub, K., Mohrig, D., and Reinhardt, L.: The unreasonable effectiveness of  
677 stratigraphic and geomorphic experiments, *Earth-Science Rev.*, 97, 1–43, doi:  
678 10.1080/17445647.2014.912036, 2009.

679 Paterson, W. S. B., Pergamon Kidlington, *The Physics of Glaciers*, Elsevier Science Ltd,  
680 Great Britain, 480 pages, 1994.

681 Patterson, C. J.: Southern Laurentide ice lobes were created by ice streams: Des Moines Lobe  
682 in Minnesota, USA, *Sediment. Geol.*, 111, 249–261, doi: 10.1016/S0037-0738(97)00018-3,  
683 1997.

684 Payne, A. J., and Dongelmans, P. W.: Self-organization in the thermomechanical flow of ice  
685 sheets. *J. Geophys. Res. Solid Earth.*, 102, 12219–12233,doi: 10.1029/97JB00513, 1997.

686

687 Perol, T., and Rice, J. R.: Shear heating and weakening of the margins of West Antarctic ice  
688 streams, *Geophys. Res. Lett.*, 42, 3406–3413, doi: 10.1002/2015GL063638, 2015.

689

690 Peters, L. E., Anandakrishnan, S., Alley, R. B., and Smith, A. M., Extensive storage of basal  
691 meltwater in the onset region of a major West Antarctic ice stream, *Geology.*, 35, 251–254,  
692 doi: 10.1130/G23222A.1, 2007.

693 Ravier, E., Buoncristiani, J. F., Menzies, J., Guiraud, M., Clerc, S., and Portier, E.: Does  
694 porewater or meltwater control tunnel valley genesis? Case studies from the Hirnantian of  
695 Morocco, *Palaeogeogr. Palaeoclimatol. Palaeoecol.*, 418, 359–376, doi:  
696 10.1016/j.palaeo.2014.12.003, 2015.

697 Raymond, C. F.: How do glaciers surge? A review, *J. Geophys. Res. Solid Earth.*, 92, 9121–  
698 9134, doi: 10.1029/JB092iB09p09121, 1987.

699 Retzlaff, R., and Bentley, C. R.: Timing of stagnation of Ice Stream C, West Antarctica, from  
700 short-pulse radar studies of buried surface crevasses, *J. Glaciol.*, 39, 553–561, doi:  
701 10.3189/S0022143000016440, 1993.

702 Robel, A. A., Degiuli, E., Schoof, C., and Tziperman, E.: Dynamics of ice stream temporal  
703 variability : Modes, scales, and hysteresis, *J. of Geophys. Res. Earth Surface.*, 118, 925–936,  
704 doi: 10.1002/jgrf.20072, 2013.

705  
706 Rothlisberger, H., and Lang, H., *Glacial hydrology. Glacio-Fluvial Sediment Transfer: An  
707 Alpine Perspective*, Gurnell and Clark, John Wiley and Sons, New York New York. p 207-  
708 284, 1987.

709 Shreve, R. L.: Movement of water in glaciers, *Journal of Glaciology.*, 11(62), 205-214, doi:  
710 10.3189/S002214300002219X, 1972.

711 Siegfried, M. R., Fricker, H. A., Carter, S. P., and Tulaczyk, S.: Episodic ice velocity  
712 fluctuations triggered by a subglacial flood in West Antarctica, *Geophys. Res. Lett.*, 43, 2640–  
713 2648, doi: 10.1002/2016GL067758, 2016.

714  
715 Stearns, L. A., Smith, B. E., and Hamilton, G. S.: Increased flow speed on a large East Antarctic  
716 outlet glacier caused by subglacial floods, *Nat. Geosci.*, 1, 827–831, doi: 10.1038/ngeo356,  
717 2008.

718  
719 Vaughan, D. G., Corr, H. F. J., Smith, A. M., Pritchard, H. D., and Shepherd, A.: Flow-  
720 switching and water piracy between Rutford Ice Stream and Carlson Inlet, West Antarctica.  
721 *Journal of Glaciology.*, 54, 41–48, doi: 10.3189/002214308784409125, 2008.

722 Vaughan, D.G., J.C. Comiso, I. Allison, J. Carrasco, G. Kaser, R. Kwok, P. Mote, T. Murray,  
723 F. Paul, J. Ren, E. Rignot, O. Solomina, K. Steffen and T. Zhang, 2013: Observations:  
724 Cryosphere. In: *Climate Change 2013: The Physical Science Basis. Contribution of Working  
725 Group I to the Fifth Assessment Report of the Intergovernmental Panel on Climate Change*  
726 [Stocker, T.F., D. Qin, G.-K. Plattner, M. Tignor, S.K. Allen, J. Boschung, A. Nauels, Y. Xia,  
727 V. Bex and P.M. Midgley (eds.)]. Cambridge University Press, Cambridge, United Kingdom  
728 and New York, NY, USA  
729

730 Winsborrow, M. C. M., Clark, C. D., and Stokes, C. R.: What controls the location of ice  
731 streams?, *Earth-Science Rev.*, 103, 45–59, doi: 10.1016/j.earscirev.2010.07.003, 2010.